

# Cross sections for electron scattering from selected components of DNA and RNA

Paweł Mozejko<sup>a,b,\*</sup>, Léon Sanche<sup>a</sup>

<sup>a</sup>*Groupe en Sciences des Radiations, Faculté de Médecine, Université de Sherbrooke, Sherbrooke, Quebec, Canada J1H5N4*

<sup>b</sup>*Atomic Physics Division, Faculty of Applied Physics and Mathematics, Gdańsk University of Technology, 870-952 Gdańsk, Poland*

Received 9 August 2004; received in revised form 22 October 2004; accepted 26 October 2004

## Abstract

Differential and integral cross sections for elastic collisions between electrons and selected analogues of components of the backbone of deoxyribonucleic acid (DNA) and ribonucleic acid (RNA) are calculated using the independent atom method with a static-polarization model potential. They are presented for tetrahydrofuran, 3-hydroxytetrahydrofuran,  $\alpha$ -tetrahydrofurfuryl alcohol, and phosphoric acid within 50–2000 eV electron energy range. Cross sections for electron-impact ionization of these molecular targets are also derived using the binary-encounter-Bethe model in the energy range from the ionization threshold to 4000 eV. Single electron-impact ionization cross sections for the sugar-phosphate unit are also approximately derived. The results are compared with available data.

© 2004 Elsevier Ltd. All rights reserved.

PACS: 34.80

**Keywords:** DNA; RNA; Sugar-phosphate backbone; Tetrahydrofuran; 3-hydroxytetrahydrofuran;  $\alpha$ -tetrahydrofurfuryl alcohol; Phosphoric acid; Ionizing radiation; Damage to DNA and RNA; Electron scattering; Elastic electron scattering; Electron impact ionization

## 1. Introduction

Monte Carlo track structure codes, such as, e.g., CPA100, OREC, PARTRAC, NOREC, (Terrissol and Beaudré, 1990; Ritchie et al., 1991; Friedland et al., 1998, 1999; Semenenko et al., 2003), and many others provide very useful tools to study damage to living cells induced by ionizing radiation (i.e.  $\beta$ -rays, X-rays, or  $\gamma$ -rays). In such simulations, the transport and energy deposition of primary particles and secondary species,

including electrons, through the cellular environment is investigated. While DNA targets are represented by models of different order of complexity (Nikjoo et al., 1999; Bernhardt et al., 2003), it is often assumed that cross section, per valence orbital, for electron interactions with DNA differs only slightly from those for liquid water (Friedland et al., 1998, 1999; Nikjoo et al., 1999; Bernhardt and Paretzke, 2003; Moissenko et al., 1998). Consequently, the input data sets include, mainly, cross sections for interactions of primary particles and secondary electrons with water in liquid and/or gaseous phase (Uehara et al., 1999). However, it has been shown that for collision energies below 250 eV, electron-impact ionization cross section of liquid water per valence electron is smaller than that of DNA (Bernhardt and Paretzke, 2003). Moreover, recent studies on low- and

\*Corresponding author. Nuclear Medicine and Radiobiology, 3001, 12 Avenue Nord, Sherbrooke, Canada J1H 5N4. Tel.: +1 819 564 5403; fax: +1 819 564 5442.

E-mail address: [Pawel.Mozejko@USherbrooke.ca](mailto:Pawel.Mozejko@USherbrooke.ca) (P. Mozejko).

intermediate-energy electron collisions with DNA and its constituents have shown that such projectiles can induce significant damage to DNA, including single- and double-strand breaks (Folkard et al., 1993; Boudaiffa 2000a, b; Sanche, 2002; Huels et al., 2003). Such breaks in DNA and its constituents can be induced via both direct and resonance interactions (Huels et al., 2003; Abdoul-Carime et al., 2001; Barrios et al., 2002; Pan et al., 2003; Li et al., 2003; Abdoul-Carime et al., 2004; Feil et al., 2004; Ptasińska et al., 2004). The former creates ionization and dissociative states, which can break the backbone. Resonances (i.e. transient anions) can decay to dissociative neutral states, but transient anions can also dissociate into neutral and anionic fragments (Huels et al., 2003; Abdoul-Carime et al., 2001; Barrios et al., 2002; Pan et al., 2003; Li et al., 2003; Abdoul-Carime et al., 2004; Feil et al., 2004; Ptasińska et al., 2004). Thus, a detailed description of the interaction of all primary and the secondary species, including low- and intermediate-energy electrons, with complex biomolecular systems are necessary for a complete description and understanding of ionizing radiation damage to DNA, RNA and living cells. As a consequence, the complete set of cross sections for electron collision with DNA and RNA and/or its building blocks are needed as input data in Monte Carlo analysis.

Up to now only few cross sections for electron interaction with DNA and RNA bases can be found in the literature. Electron impact ionization cross sections for adenine, cytosine, guanine, thymine and the sugar-phosphate backbone have been calculated using Deutsch-Märk (DM) and the Binary-Encounter-Bethe (BEB) formalisms for an energy range between the ionization threshold and 1 keV by Bernhardt and Paretzke (Bernhardt and Paretzke, 2003). Recently, we have presented differential and integral elastic cross sections for electron scattering by the purine (adenine and guanine) and pyrimidine (thymine, cytosine and uracil) bases calculated with the independent atom method (IAM) for collision energies ranging from 50 to 4000 eV (Mozejko and Sanche, 2003)<sup>1</sup>. For the same targets, using the BEB formalism, we have calculated electron impact ionization cross sections for energies between the ionization threshold and 5 keV (Mozejko and Sanche, 2003). Very recently, absolute partial cross sections for positive and negative ion formation by electron impact on uracil have been measured and reported (Feil et al., 2004). In the same work, normalized total single ionization cross sections have been presented for uracil. Inelastic electron interactions with

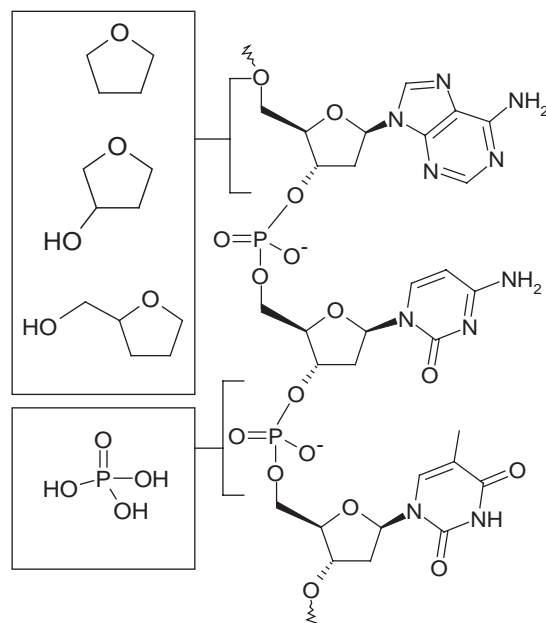


Fig. 1. A short-chain segment of the single-stranded deoxyribose backbone of DNA and chemical structure of molecules investigated.

2-deoxy-*D* ribose (deoxyribose) have been studied with a monochromatic electron beam and a quadrupole mass spectrometer by Ptasińska et al. (2004). While cross sections for the formation of some negative ions via dissociative electron attachment to deoxyribose have been recorded on an absolute scale, the positive ion yields have been presented only in the arbitrary units (Ptasińska et al., 2004).

The objective of the present study is to provide reliable elastic and ionization cross sections for electron scattering from molecules, which due to their structure and/or functional groups, are similar to those found in the backbone of DNA and RNA (Fig. 1). As analogues of the sugar in the sugar-phosphate backbone, we chose tetrahydrofuran (C<sub>4</sub>H<sub>8</sub>O), 3-hydroxytetrahydrofuran (C<sub>4</sub>H<sub>8</sub>O<sub>2</sub>) and  $\alpha$ -tetrahydrofurfuryl alcohol (C<sub>5</sub>H<sub>10</sub>O<sub>2</sub>). As analogues of the phosphate group we have studied phosphoric acid (H<sub>3</sub>PO<sub>4</sub>). The chemical structures of these molecules are shown in Fig. 1 with an indication to the corresponding segments of the backbone. For comparison, elastic integral cross sections for electron scattering from tetraphosphorus hexoxide (P<sub>4</sub>O<sub>6</sub>) and phosphorus (III) oxide (P<sub>2</sub>O<sub>3</sub>) have also been calculated.

## 2. Computational procedures

The theoretical approach and computational procedures applied in the present work are essentially the same as those used in our previous calculations

<sup>1</sup>Please note that due to some typographical errors, the elastic cross sections given in the last row (Energy = 4000 eV) in Table 4 in (Mozejko and Sanche, 2003) are incorrect. They should read 2.943 for guanine, 2.712 for adenine, 2.481 for thymine, 2.207 for cytosine and 2.128 for uracil.

(Mozejko and Sanche, 2003; Mozejko et al., 2002). Thus, only a short description of the methods and procedures is given here.

Elastic cross sections between 50 and 2000 eV have been calculated with the IAM (Mott and Massey, 1965) with a static + polarization model potential. In this method, electron-molecule collisions are reduced to electron interactions with individual atoms of the target molecule. This reduction is based on the following assumptions: (i) each atom of the molecule scatters independently; (ii) redistribution of atomic electrons due to molecular binding is unimportant; and (iii) multiple scattering within the molecule is negligible (Mott and Massey, 1965). It has been shown that IAM can provide reasonable results only above about 50 eV (e.g. see (Mozejko et al., 2002; Joshipura and Vinodkumar, 1997; Maji et al., 1998) and references therein).

In the IAM method, the differential cross section (DCS) for elastic electron scattering on a molecule, taking into account all possible orientations of the intermolecular axis in the space, is given as

$$\frac{d\sigma}{d\Omega} = \sum_i^N \sum_j^N f_i(\theta, k) f_j^*(\theta, k) \frac{\sin(sr_{ij})}{sr_{ij}}, \quad (1)$$

where  $N$  is the number of atoms within a molecule,  $\theta$  is the scattering angle and  $f_i(\theta, k)$  and  $f_j(\theta, k)$  are complex scattering amplitudes due to the  $i$ th and  $j$ th atom of the molecule, respectively.  $s = 2k \sin(\theta/2)$  is the magnitude of the momentum transfer during the collision and  $k = \sqrt{2E}$  is the wave number of the incident electron. The distance between the  $i$ th and  $j$ th atom is denoted as  $r_{ij}$ . In all equations, regarding elastic scattering, we adopted atomic units in which  $e = m = \hbar = 1$ , although all presented and discussed results of our calculation are given in the SI units. The distances  $r_{ij}$  between atoms of the studied molecules were obtained using the optimization procedure of the GAMESS code (Schmidt et al., 1993).

The integral cross section for elastic scattering is given by

$$\sigma(E) = \frac{4\pi}{k} \sum_{i=1}^N \text{Im} f_i(\theta = 0, k) = \sum_i^N \sigma_i(E), \quad (2)$$

where  $\sigma_i(E)$  is the integral elastic cross section of the  $i$ th atom of the target molecule and  $E$  is the energy of the incident electron.

We obtained the elastic electron-atom cross sections and atomic scattering amplitudes by partial wave analysis and solved numerically the radial Schrödinger equation

$$\left( \frac{d^2}{dr^2} - \frac{l(l+1)}{r^2} - 2(V_{\text{stat}}(r) + V_{\text{polar}}(r)) + k^2 \right) u_l(r) = 0 \quad (3)$$

under the boundary conditions

$$u_l(0) = 0, \quad u_l(r) \xrightarrow{r \rightarrow \infty} A_l \hat{j}_l(kr) - B_l \hat{n}_l(kr), \quad (4)$$

where  $\hat{j}_l(kr)$  and  $\hat{n}_l(kr)$  are the spherical Bessel–Riccati and Neumann–Riccati functions, respectively.  $V_{\text{stat}}(r)$  is the static potential expressed in the form proposed by Salvat et al. (1987). The polarization potential  $V_{\text{polar}}(r)$  was expressed in the form proposed by Padial and Norcross (1984)

$$V_{\text{polar}}(r) = \begin{cases} v(r), & r \leq r_c \\ -\alpha/2r^4, & r > r_c \end{cases}, \quad (5)$$

where  $v(r)$  is the free-electron-gas correlation energy (Pedrew and Zunger, 1981) and  $\alpha$  is the static electric dipole polarizability of atom.  $r_c$  is the first crossing point of the  $v(r)$  and  $-\alpha/2r^4$  curves (Zhang et al., 1992). The phase shifts  $\delta_l$  are connected to the asymptotic form of the wave function,  $u_l(r)$ , by

$$\tan \delta_l = \frac{B_l}{A_l}. \quad (6)$$

Electron-impact ionization cross sections have been obtained within the binary-encounter-Bethe (BEB) formalism (Hwang et al., 1996). Within this formalism the electron-impact ionization cross section per molecular orbital is given by

$$\sigma^{\text{BEB}} = \frac{S}{t+u+1} \left[ \frac{\ln t}{2} \left( 1 - \frac{1}{t^2} \right) + 1 - \frac{1}{t} - \frac{\ln t}{t+1} \right], \quad (7)$$

where  $u = U/B$ ,  $t = T/B$ ,  $S = 4\pi a_0^2 N R^2 / B^2$ ,  $a_0 = 0.5292 \text{ \AA}$ ,  $R = 13.61 \text{ eV}$ , and  $T$  is the energy of impinging electrons. Finally, the total cross section for electron-impact ionization,  $\sigma_{\text{ion}}$ , was obtained as the sum of  $\sigma^{\text{BEB}}$  for all molecular orbitals (MO)

$$\sigma^{\text{ion}} = \sum_{i=1}^{n_{\text{MO}}} \sigma_{n_{\text{MO}}}^{\text{BEB}}. \quad (8)$$

The electron binding energy  $B$ , kinetic energy of the orbital,  $U$ , and orbital occupation number,  $N$ , were obtained for the ground states of the molecules with the Hartree–Fock method using the GAMESS code (Schmidt et al., 1993), and Gaussian 6-311G basis set. Because the valence orbital energies obtained in this way usually differ slightly from experimental ones, we performed also outer valence Green function calculations of correlated electron affinities and ionization potentials (Zakrzewski and von Niessen, 1994) with the GAUSSIAN code (Gaussian 98, 2001).

### 3. Results

#### 3.1. Elastic scattering

Results of differential elastic cross section calculations for electron collisions with  $\text{H}_3\text{PO}_4$ ,  $\text{C}_4\text{H}_8\text{O}$ ,  $\text{C}_4\text{H}_8\text{O}_2$  and  $\text{C}_5\text{H}_{10}\text{O}_2$  at energies of 50, 100, 200 and 500 eV are presented in Figs. 2(a–d), respectively. To our knowledge, there is no other experimental or theoretical data available for comparison. Generally, like for purine and pyrimidine bases (Mozejko and Sanche, 2003), the cross sections decrease with increasing electron energy. Only for small scattering angles, i.e. for forward and near-to-forward scattering, does elastic DCS increase with collision energy. The angular dependence of elastic cross sections for  $\text{C}_4\text{H}_8\text{O}$ ,  $\text{C}_4\text{H}_8\text{O}_2$  and  $\text{C}_5\text{H}_{10}\text{O}_2$  is similar, which is related to similarities in the geometry of the targets.

Integral elastic cross sections for phosphoric acid, tetrahydrofuran, 3-hydroxytetrahydrofuran and  $\alpha$ -tetrahydrofurfuryl alcohol, computed according to Eq. (2), are listed, in numerical form, at selected electron energies in Table 1. Their energy dependence between 50 and 2000 eV is shown in Figs. 3(a) and (b), respectively. It is important to note that according to the main assumption of the IAM, the magnitude of the cross section for low collision energies will be overestimated, mainly due to the neglect of bond distortion and multiple scattering within the molecule. On the other hand, for some small and intermediate size molecules like silane and germane, even for energies as low as 20 eV, the IAM method predicts reasonable elastic cross sections (Mozejko et al., 2002). On the

other hand, since in the present approach exchange and absorption effects are neglected, one can expect that resulting differential and integral cross sections can be overestimated for energies lower than 300 eV (Khare et al., 1994). For all studied molecules, the magnitude of integral elastic cross section decreases with increasing collision energy.  $\alpha$ -tetrahydrofurfuryl alcohol has the highest elastic cross section. It is about 19% and 17% higher at low- and intermediate-energies, respectively, than those for 3-hydroxytetrahydrofuran. The integral elastic cross section for tetrahydrofuran is smaller than the cross section for 3-hydroxytetrahydrofuran by more than 13%. For  $\text{H}_3\text{PO}_4$ , the integral elastic cross section is smaller than those for the sugar analogues for collision energies below 250 eV. For higher energies that cross section decreases more slowly with energy than those for  $\text{C}_4\text{H}_8\text{O}$ ,  $\text{C}_4\text{H}_8\text{O}_2$ , and  $\text{C}_5\text{H}_{10}\text{O}_2$ . Consequently, for collision energies higher than 1.1 keV the cross section for  $\text{H}_3\text{PO}_4$  molecules exceeds those for  $\text{C}_4\text{H}_8\text{O}$  and  $\text{C}_4\text{H}_8\text{O}_2$ . This energy dependence of the integral cross sections is typical of some molecules. In our case, it builds up from phosphorous and oxygen. This can be shown by examining integral elastic cross sections for larger molecules containing these atoms, such as those for  $\text{P}_2\text{O}_3$  and  $\text{P}_4\text{O}_6$  presented in Fig. 3(a). The integral elastic cross sections for  $\text{H}_3\text{PO}_4$ ,  $\text{P}_2\text{O}_3$ , and  $\text{P}_4\text{O}_6$  depends strongly on the molecular size. On the other hand, their shape at higher collision energies, especially for  $\text{H}_3\text{PO}_4$  and  $\text{P}_2\text{O}_3$  is very similar. In Fig. 4, integral elastic cross section computed for the studied targets are compared with those calculated for DNA and RNA bases (Mozejko and Sanche, 2003). In the investigated energy range, the integral cross sections for phosphoric

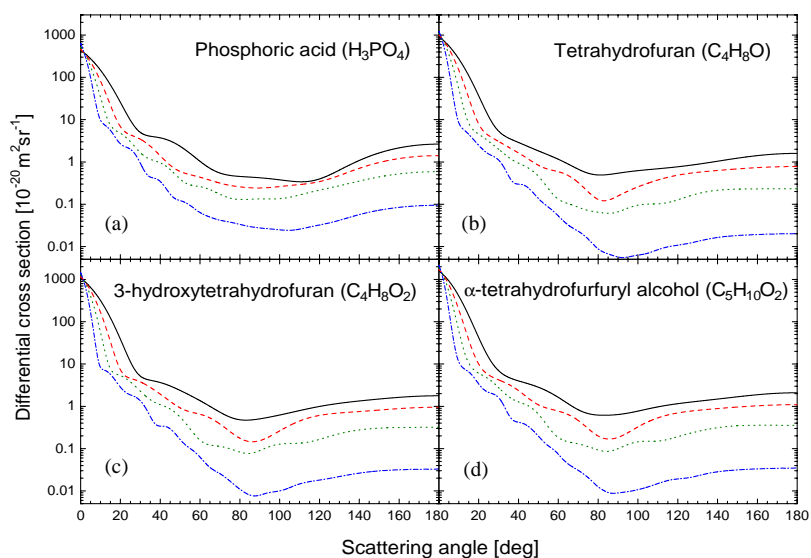


Fig. 2. Differential cross section for elastic electron collisions with studied targets at: (—) 50 eV, (---) 100 eV, (···) 200 eV and (- · -) 500 eV.

Table 1

Integral elastic cross section for electron scattering from phosphoric acid ( $\text{H}_3\text{PO}_4$ ), tetrahydrofuran ( $\text{C}_4\text{H}_8\text{O}$ ), 3-hydroxytetrahydrofuran ( $\text{C}_4\text{H}_8\text{O}_2$ ) and  $\alpha$ -tetrahydrofurfuryl alcohol ( $\text{C}_5\text{H}_{10}\text{O}_2$ ) at selected energies in units of  $10^{-20} \text{ m}^2$

Energy (eV)	$\text{H}_3\text{PO}_4$	$\text{C}_4\text{H}_8\text{O}$	$\text{C}_4\text{H}_8\text{O}_2$	$\text{C}_5\text{H}_{10}\text{O}_2$
50	27.6	31.6	35.7	42.5
60	24.0	27.4	30.9	36.9
70	21.5	24.4	27.5	32.9
80	19.6	22.1	25.0	29.8
90	18.1	20.3	23.0	27.4
100	16.9	18.9	21.3	25.4
110	16.0	17.6	19.9	23.8
120	15.1	16.6	18.8	22.4
140	13.8	14.9	16.9	20.1
160	12.7	13.6	15.4	18.3
180	11.8	12.5	14.2	16.9
200	11.1	11.6	13.2	15.7
220	10.5	10.8	12.3	14.7
250	9.71	9.86	11.3	13.4
300	8.68	8.63	9.88	11.7
350	7.88	7.67	8.83	10.5
400	7.23	6.96	8.00	9.48
450	6.70	6.36	7.32	8.67
500	6.25	5.85	6.75	7.99
600	5.52	5.06	5.86	6.93
700	4.96	4.47	5.18	6.12
800	4.52	4.00	4.65	5.49
900	4.15	3.63	4.23	4.98
1000	3.84	3.32	3.87	4.57
1100	3.58	3.07	3.58	4.22
1200	3.36	2.85	3.33	3.93
1400	3.00	2.51	2.93	3.46
1600	2.72	2.25	2.64	3.10
1800	2.50	2.06	2.40	2.83
2000	2.32	1.90	2.23	2.62

acid, tetrahydrofuran and 3-hydroxytetrahydrofuran are always smaller than those of the integral cross sections for uracil, cytosine, thymine, adenine and guanine.  $\alpha$ -tetrahydrofurfuryl alcohol, uracil and cytosine have comparable integral elastic cross section.

### 3.2. Electron impact ionization

The calculated total cross sections for single ionization by electron impact of phosphoric acid, tetrahydrofuran, 3-hydroxytetrahydrofuran and  $\alpha$ -tetrahydrofurfuryl alcohol are listed at selected energies in Table 2. The energy dependence of these cross sections is presented in Fig. 5. In the BEB calculation we have used the following energies of the first ionization potential, calculated with the GAUSSIAN code (Gaussian 98, 2001): 11.72 eV for  $\text{H}_3\text{PO}_4$ , 9.26 eV for  $\text{C}_4\text{H}_8\text{O}$ , 9.51 eV for  $\text{C}_4\text{H}_8\text{O}_2$ , and 9.47 eV for  $\text{C}_5\text{H}_{10}\text{O}_2$ .

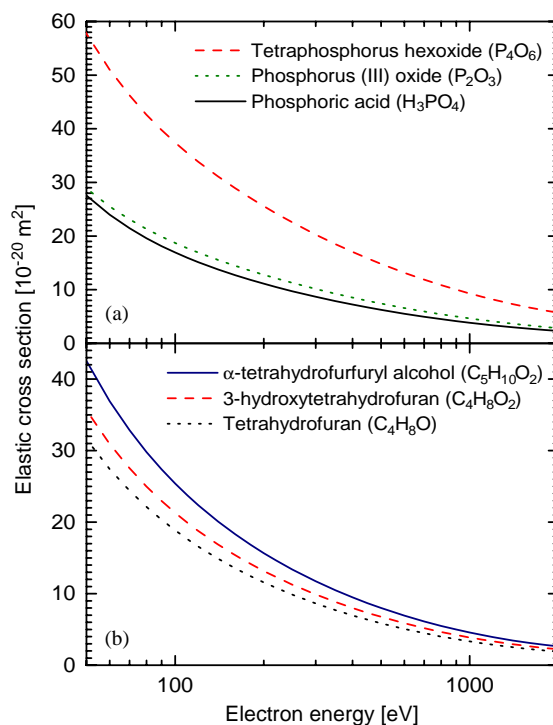


Fig. 3. Integral elastic cross section for electron collisions with studied molecules: (a)  $\text{P}_4\text{O}_6$ ,  $\text{P}_2\text{O}_3$  and  $\text{H}_3\text{PO}_4$  molecules; (b)  $\text{C}_4\text{H}_8\text{O}$ ,  $\text{C}_4\text{H}_8\text{O}_2$  and  $\text{C}_5\text{H}_{10}\text{O}_2$  molecules.

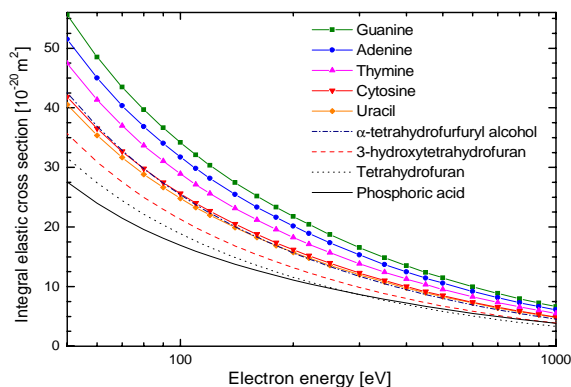


Fig. 4. Comparison of the integral elastic cross section for electron scattering from guanine, adenine, thymine, cytosine, uracil (Mozejko and Sanche, 2003),  $\alpha$ -tetrahydrofurfuryl alcohol, 3-hydroxytetrahydrofuran, tetrahydrofuran and phosphoric acid molecules.

Ionization processes induced by electrons are most efficient for  $\alpha$ -tetrahydrofurfuryl alcohol. For  $\text{C}_4\text{H}_8\text{O}$ , the cross section maximum of  $12.69 \times 10^{-20} \text{ m}^2$  is located at 75 eV. For  $\text{C}_4\text{H}_8\text{O}_2$  and  $\text{C}_5\text{H}_{10}\text{O}_2$  ionization cross section maxima of  $14.16 \times 10^{-20}$  and  $17.11 \times$

Table 2

Total cross section for electron impact ionization of phosphoric acid ( $\text{H}_3\text{PO}_4$ ), tetrahydrofuran ( $\text{C}_4\text{H}_8\text{O}$ ), 3-hydroxytetrahydrofuran ( $\text{C}_4\text{H}_8\text{O}_2$ ) and  $\alpha$ -tetrahydrofurfuryl alcohol  $\text{C}_5\text{H}_{10}\text{O}_2$  at selected energies in units of  $10^{-20} \text{ m}^2$

Energy (eV)	$\text{H}_3\text{PO}_4$	$\text{C}_4\text{H}_8\text{O}$	$\text{C}_4\text{H}_8\text{O}_2$	$\text{C}_5\text{H}_{10}\text{O}_2$
12.0	0.0313	0.370	0.432	0.500
13.0	0.155	0.740	0.771	1.006
14.0	0.377	1.161	1.230	1.575
15.0	0.676	1.627	1.746	2.219
16.0	1.025	2.167	2.303	2.922
17.0	1.397	2.721	2.890	3.636
18.0	1.770	3.300	3.485	4.385
19.0	2.131	3.852	4.082	5.114
20.0	2.476	4.375	4.651	5.806
22.5	3.281	5.557	5.944	7.388
25.0	4.040	6.634	7.121	8.802
27.5	4.727	7.554	8.136	10.04
30	5.329	8.366	9.034	11.12
35	6.311	9.670	10.49	12.86
40	7.077	10.63	11.57	14.16
45	7.701	11.32	12.39	15.12
50	8.188	11.82	12.99	15.81
55	8.564	12.18	13.42	16.31
60	8.852	12.41	13.72	16.66
65	9.071	12.57	13.93	16.89
70	9.234	12.65	14.06	17.03
75	9.351	12.69	14.14	17.10
80	9.433	12.69	14.16	17.11
85	9.484	12.65	14.15	17.09
90	9.511	12.60	14.11	17.02
95	9.519	12.52	14.05	16.94
100	9.510	12.43	13.97	16.83
110	9.454	12.21	13.76	16.56
120	9.362	11.97	13.52	16.26
140	9.113	11.46	13.00	15.60
160	8.822	10.94	12.45	14.92
180	8.520	10.45	11.92	14.26
200	8.220	9.980	11.41	13.64
225	7.858	9.442	10.82	12.93
250	7.517	8.954	10.28	12.27
275	7.200	8.511	9.789	11.68
300	6.903	8.109	9.339	11.13
350	6.376	7.411	8.555	10.19
400	5.922	6.827	7.894	9.394
450	5.529	6.331	7.331	8.718
500	5.186	5.906	6.846	8.138
600	4.619	5.214	6.055	7.191
700	4.168	4.675	5.436	6.453
800	3.802	4.242	4.938	5.859
900	3.499	3.888	4.528	5.371
1000	3.243	3.591	4.186	4.963
1500	2.393	2.621	3.061	3.626
2000	1.911	2.080	2.432	2.880
2500	1.598	1.733	2.027	2.399
3000	1.377	1.489	1.743	2.063
3500	1.213	1.309	1.533	1.814
4000	1.085	1.170	1.370	1.621

$10^{-20} \text{ m}^2$ , respectively, are peaked at 80 eV. Among all studied targets phosphoric acid has the lowest ionization cross section, with a maximum of  $9.52 \times 10^{-20} \text{ m}^2$  at 95 eV.

Fig. 6 shows comparison between total cross sections for electron-impact ionization of DNA and RNA bases (i.e. guanine, adenine, thymine, cytosine and uracil) (Mozejko and Sanche, 2003) and those for ionization of  $\text{C}_4\text{H}_8\text{O}$ ,  $\text{C}_4\text{H}_8\text{O}_2$ ,  $\text{C}_5\text{H}_{10}\text{O}_2$  and  $\text{PO}_4\text{H}_3$  for electron energies from the ionization threshold to 120 eV. With exception of some specific variation of the cross sections near the ionization threshold, generally, in the whole energy range investigated, the magnitude of the ionization cross section obeys the following trend:

$$\sigma_{\text{PO}_4\text{H}_3} < \sigma_{\text{C}_4\text{H}_8\text{O}} < \sigma_{\text{C}_4\text{H}_8\text{O}_2} < \sigma_{\text{uracil}} < \sigma_{\text{cytosine}} < \sigma_{\text{C}_5\text{H}_{10}\text{O}_2} < \sigma_{\text{thymine}} < \sigma_{\text{adenine}} < \sigma_{\text{guanine}}. \quad (9)$$

It has been shown that, in some cases and within some approximation the electron-impact ionization cross section for polyatomic molecules can be calculated taking into account only basic atomic properties (Margreiter et al., 1990). From this assumption, we approximate ionization cross sections for the sugar-phosphate backbone of DNA adding ionization cross sections for  $\text{H}_3\text{PO}_4$  and  $\text{C}_5\text{H}_{10}\text{O}_2$ . In Fig. 7 the resulting values are compared with recent calculations by Bernhardt and Paretzke (Bernhardt and Paretzke, 2003) of ionization cross sections for the sugar-phosphate unit of DNA. At low (i.e. near to the ionization threshold) energies, the magnitude of the summed cross sections is distinctively overestimated for sugar-phosphate unit (at 20 eV it is higher of more than 27%), but at higher energies discrepancies between both cross sections are reasonably smaller. While summed ionization cross section is always higher than those calculated for the sugar-phosphate unit, discrepancies do not exceed 10% at 30 eV and become smaller with increasing electron energies. At 1 keV both cross section differ by less than 7%.

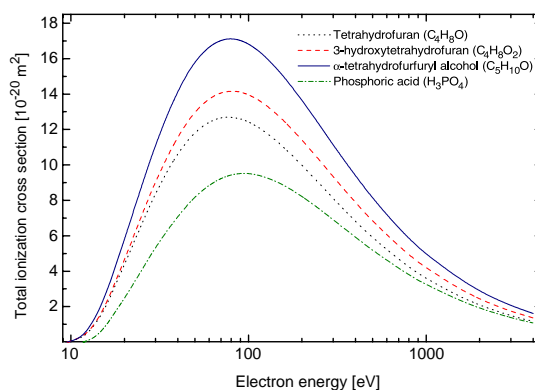


Fig. 5. Electron-impact ionization cross section for  $\text{H}_3\text{PO}_4$ ,  $\text{C}_4\text{H}_8\text{O}$ ,  $\text{C}_4\text{H}_8\text{O}_2$  and  $\text{C}_5\text{H}_{10}\text{O}_2$  molecules.

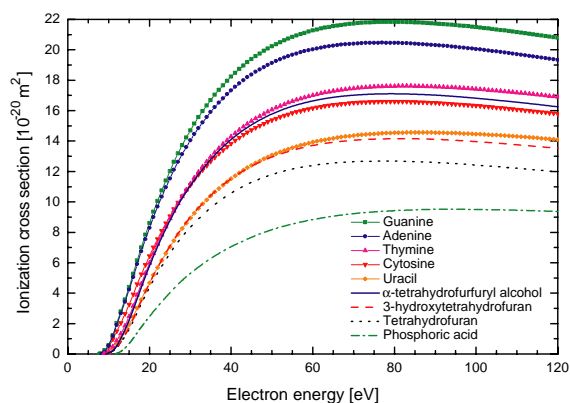


Fig. 6. Comparison of the electron-impact ionization cross section for guanine, adenine, thymine, cytosine, uracil (Mozejko and Sanche, 2003),  $\alpha$ -tetrahydrofurfuryl alcohol, 3-hydroxytetrahydrofuran, tetrahydrofuran and phosphoric acid molecules.

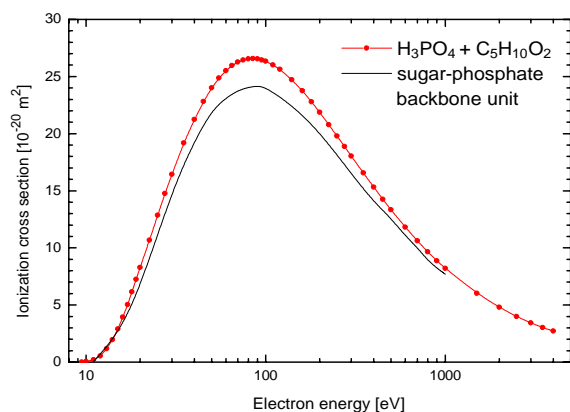


Fig. 7. Comparison between cross section for electron impact ionization of the sugar-phosphate backbone unit with the sum of electron-impact ionization cross sections of phosphoric acid and  $\alpha$ -tetrahydrofurfuryl alcohol.

#### 4. Summary

Using relatively simple but reliable approaches, i.e. the independent atom method and binary-encounter-Bethe formalism, cross sections for elastic electron collisions and electron-impact ionization from  $C_4H_8O$ ,  $C_4H_8O_2$ ,  $C_5H_{10}O_2$  and  $H_3PO_4$  have been computed for wide range of the collision energies. The cross section for electron-impact ionization of the sugar phosphate unit of DNA has been approximated as the sum of the ionization cross section of the  $H_3PO_4$  and  $C_5H_{10}O_2$  molecules. We found reasonable agreement with results of more sophisticated calculations for energies higher than 30 eV. The present results can be useful in a detailed analysis of ionizing radiation damage to

complex biomolecules such as DNA and RNA, via Monte Carlo simulations.

#### Acknowledgements

This work was supported by the Canadian Institutes of Health Research (CIHR). Paweł Mozejko acknowledges financial support from the CIHR in the form of a Post-doctoral Fellowship.

#### References

- Abdoul-Carime, H., Cloutier, P., Sanche, L., 2001. Low-energy (5–40 eV) electron-stimulated desorption of anions from physisorbed DNA bases. *Radiat. Res.* 155, 633–645.
- Abdoul-Carime, H., Gohlke, S., Illenberger, E., 2004. Site-specific dissociation of DNA bases by slow electrons at early stages of irradiation. *Phys. Rev. Lett.* 92 (16), 168103.
- Barrios, R., Skurski, P., Simons, J., 2002. Mechanism for damage to DNA by low-energy electrons. *J. Phys. Chem. B* 106, 7991–7994.
- Bernhardt, Ph., Paretzke, H.G., 2003. Calculation of electron impact ionization cross section of DNA using the Deutsch-Märk and Binary-Encounter-Bethe formalisms. *Int. J. Mass Spectrom.* 223–224, 599–611.
- Bernhardt, Ph., Friedland, W., Jacob, P., Paretzke, H.G., 2003. Modeling of ultrasoft X-ray induced DNA damage using structured higher order DNA targets. *Int. J. Mass Spectrom.* 223/224, 579–597.
- Boudaiffa, B., Cloutier, P., Hunting, D., Huels, M.A., Sanche, L., 2000a. Resonant formation of DNA strand breaks by low-energy (3–20 eV) electrons. *Science* 287, 1658–1660.
- Boudaiffa, B., Hunting, D., Cloutier, P., Huels, M.A., Sanche, L., 2000b. Induction of single- and double-strand breaks in plasmid DNA by 100–1500 eV electrons. *Int. J. Radiat. Biol.* 76, 1209–1221.
- Feil, S., Gluch, K., Matt-Lebner, S., Scheier, P., Limtrakul, J., Probst, M., Deutsch, H., Becker, K., Stamatovic, A., Märk, T.D., 2004. Partial cross sections for positive and negative ion formation following electron impact on uracil. *J. Phys. B* 37, 3013–3020.
- Folkard, M., Prise, K.M., Vojnovic, B., Davies, S., Roper, M.J., Michael, B.D., 1993. Measurement of DNA damage by electrons with energies between 25 and 4000 eV. *Int. J. Radiat. Biol.* 64, 651–658.
- Friedland, W., Jacob, P., Paretzke, H.G., Stork, T., 1998. Monte Carlo simulation of the production of short DNA fragments by low-linear energy transfer radiation using higher-order DNA models. *Radiat. Res.* 150, 170–182.
- Friedland, W., Jacob, P., Paretzke, H.G., Merzagora, M., Ottolenghi, A., 1999. Simulation of DNA fragment distributions after irradiation with photons. *Radiat. Environ. Biophys.* 38, 39–47.
- Gaussian, 98, Revision A.11.2, Frisch, M.J., Trucks, G.W., Schlegel, H.B., Scuseria, G.E., Robb, M.A., Cheeseman, J.R., Zakrzewski, V.G., Montgomery Jr., J.A., Stratmann, R.E., Burant, J.C., Dapprich, S., Millam, J.M., Daniels, A.D., Kudin, K.N., Strain, M.C., Farkas, O., Tomasi, J.,

- Barone, V., Cossi, M., Cammi, R., Mennucci, B., Pomelli, C., Adamo, C., Clifford, S., Ochterski, J., Petersson, G.A., Ayala, P.Y., Cui Q., Morokuma, K., Rega, N., Salvador, P., Dannenberg, J.J., Malick, D.K., Rabuck, A.D., Raghavachari, K., Foresman, J.B., Cioslowski, J., Ortiz, J.V., Baboul, A.G., Stefanov, B.B., Liu, G., Liashenko, A., Piskorz, P., Komaromi, I., Gomperts, R., Martin, R.L., Fox, D.J., Keith, T., Al-Laham, M.A., Peng, C.Y., Nanayakkara, A., Challacombe, M., Gill, P.M.W., Johnson, B., Chen, W., Wong, M.W., Andres, J.L., Gonzalez, C., Head-Gordon, M., Replegle, E.S., Pople, J.A., Gaussian, Inc., Pittsburgh PA, 2001.
- Huels, M.A., Boudaiffa, B., Cloutier, P., Hunting, D., Sanche, L., 2003. Single, double and multiple double strand breaks induced in DNA by 3–100 eV electrons. *J. Am. Chem. Soc.* 125, 4467–4477.
- Hwang, W., Kim, Y.K., Rudd, M.E., 1996. New model for electron-impact ionization cross sections of molecules. *J. Chem. Phys.* 104, 2956–2966.
- Joshiyura, K.N., Vinodkumar, M., 1997. Total cross sections of electron collisions with S atoms: H<sub>2</sub>S, OCS and SO<sub>2</sub> molecules ( $E_i \geq 50$  eV). *Z. Phys. D* 41, 133–137.
- Khare, S.P., Raj, D., Sinha, P., 1994. Absorption effects in the elastic scattering of electrons by the CF<sub>4</sub> molecule at intermediate energies. *J. Phys. B* 27 (12), 2569–2576.
- Li, X.F., Sevilla, M.D., Sanche, L., 2003. Density functional theory studies of electron interaction with DNA: Can zero eV electrons induce strand breaks? *J. Am. Chem. Soc.* 125 (45), 13668–13669.
- Maji, S., Basavaraju, G., Bharathi, S.M., Bhushan, K.G., Khare, S.P., 1998. Elastic scattering of electrons by polyatomic molecules in the energy range 300–1300 eV: CO, CO<sub>2</sub>, CH<sub>4</sub>, C<sub>2</sub>H<sub>4</sub> and C<sub>2</sub>H<sub>6</sub>. *J. Phys. B* 31, 4975–4990.
- Margreiter, D., Deutsch, H., Schmidt, M., Märk, T.D., 1990. Electron impact ionization cross sections of molecules. Part II. Theoretical determination of total (counting) ionization cross sections of molecules: a new approach. *Int. J. Mass Spectrom. Ion Proc.* 100, 157–176.
- Moissenko, V.V., Hamm, R.N., Walker, A.J., Rrestwich, W.V., 1998. Modelling DNA damage induced by different energy photons and tritium beta-particles. *Int. J. Radiat. Biol.* 74, 533–550.
- Mott, N.F., Massey, H.S.W., 1965. *The Theory of Atomic Collisions*. Oxford University Press, Oxford.
- Mozejko, P., Sanche, L., 2003. Cross section calculations for electron scattering from DNA and RNA bases. *Radiat. Environ. Biophys.* 42 (3), 201–211.
- Mozejko, P., Żywicka-Mozejko, B., Szymkowski, Cz., 2002. Elastic cross section calculations for electron collisions with XY<sub>4</sub> (X = Si, Ge; Y = H, F, Cl, Br, I) molecules. *Nucl. Instr. and Meth. Phys. Res. B* 196, 245–252.
- Nikjoo, H., O'Neill, P., Terrissol, M., Goodhead, D.T., 1999. Quantitative modelling of DNA damage using Monte Carlo track structure method. *Radiat. Environ. Biophys.* 38, 31–38.
- Padial, N.T., Norcross, D.W., 1984. Parameter-free model of the correlation-polarization potential for electron-molecule collisions. *Phys. Rev. A* 29, 1742–1748.
- Pan, X., Cloutier, P., Hunting, D., Sanche, L., 2003. Dissociative electron attachment to DNA. *Phys. Rev. Lett.* 90, 208102/1–208102/4.
- Pedrew, J.P., Zunger, A., 1981. Self-interaction correction to density-functional approximations for many-electron systems. *Phys. Rev. B* 23, 5048–5079.
- Ptasińska, S., Denfil, S., Scheier, P., Märk, T.D., 2004. Inelastic electron interaction (attachment/ionization with) deoxyribose. *J. Chem. Phys.* 120 (18), 8505–8511.
- Ritchie, R.H., Hamm, R.N., Turner, J.E., Wright, H.A., Bloch, W.E., 1991. Radiation interactions and energy transport in the condensed phase. In: Glass, W.A., Varma, N.M. (Eds.), *Physical and Chemical Mechanisms in Molecular Radiation Biology*. Plenum Press, New York, pp. 99–135.
- Salvat, F., Martinez, J.D., Mayol, R., Parellada, J., 1987. Analytical Dirac–Hartree–Fock–Slater screening function for atoms ( $Z = 1–92$ ). *Phys. Rev. A* 36, 467–474.
- Sanche, L., 2002. Nanoscopic aspects of radiobiological damage: fragmentation induced by secondary electrons. *Mass Spectrom. Rev.* 21, 349–369.
- Schmidt, M.W., Baldrige, K.K., Boatz, J.A., Elbert, S.T., Gordon, M.S., Jensen, J.H., Koseki, S., Matsunaga, N., Nguyen, K.A., Su, S., Windus, T.L., Dupuis, M., Montgomery Jr., J.A., 1993. General atomic and molecular electronic structure system. *J. Comp. Chem.* 14, 1347–1363.
- Semenenko, V.A., Turner, J.E., Borak, T.B., 2003. NOREC, a Monte Carlo code for simulating electron tracks in liquid water. *Radiat. Environ. Biophys.* 42 (3), 213–217.
- Terrissol, M., Beaudré, A., 1990. Simulation of space and time evolution of radiolytic species induced by electrons in water. *Radiat. Prot. Dosim.* 31, 171–175.
- Uehara, S., Nikjoo, H., Goodhead, D.T., 1999. Comparison and assessment of electron cross sections for Monte Carlo track structure codes. *Radiat. Res.* 152, 202–213.
- Zakrzewski, V.G., von Niessen, W., 1994. Vectorizable algorithm for Green function and many-body perturbation methods. *J. Comp. Chem.* 14, 13–18.
- Zhang, X., Sun, J., Liu, Y., 1992. A new approach to the correlation polarization potential–low-energy electron elastic scattering by He atoms. *J. Phys. B* 25, 1893–1897.